

AN ABSTRACT OF THE THESIS OF

Kendall Lyman Carder for the M. S. in Oceanography (Physical)
(Name) (Degree) (Major)

Date thesis is presented September 28, 1966

Title: ERROR ANALYSIS OF INTERFEROMETRY IN MEASURE-
MENT OF FORWARD SCATTER IN SEAWATER

Abstract approved Redacted for Privacy
(Major professor)

An interferometric method of studying the forward scatter of light is proposed and analyzed. This study demonstrates that a single-mode, spacially coherent laser is necessary as a light source. Techniques are proposed to find the volume scattering function, $\beta(\theta)$, for $\theta = 0^\circ$, and an error analysis of these methods using the latest equipment is made. In addition, a scheme is suggested to compare the polarization of light scattered in the forward direction by seawater with the theoretical polarization of light as determined by Mie theory.

Equipment noise prevents an adequate signal-to-noise ratio for the determination of $\beta(0^\circ)$, but the study of the polarization of light scattered in the forward direction can be made within certain limits and compared to theoretical Mie scatter.

ERROR ANALYSIS OF INTERFEROMETRY IN
MEASUREMENT OF FORWARD SCATTER
IN SEAWATER

by

KENDALL LYMAN CARDER

A THESIS

submitted to

OREGON STATE UNIVERSITY

in partial fulfillment of
the requirements for the
degree of

MASTER OF SCIENCE

June 1967

APPROVED:

Redacted for Privacy

Associate Professor of Oceanography

In Charge of Major

Redacted for Privacy

Head of Department of Oceanography

Redacted for Privacy

Dean of Graduate School

Date thesis is presented September 28, 1966

Typed by Opal Grossnicklaus

TABLE OF CONTENTS

I. INTRODUCTION	1
The Volume Scattering Function	2
Total Scattering Coefficient	6
II. A METHOD PROPOSED TO FIND $\beta(0^\circ)$	8
Interferometry in Scatter Measurements	8
Conventional Light Sources	10
The Non-monochromaticity of Conventional	
Light Sources	10
The Incoherency of Conventional Light	
Sources	11
The Non-parallelity of Conventional	
Light Sources	14
Laser Sources	15
Mie Scattering Theory	16
Distinguishing Various Types of Particles	19
Separating the Unscattered Light from that	
Light Scattered Forward ($\theta=0^\circ$)	21
Adjusting $E_{c.b.}$ to Obtain Destructive	
Interference with $E_{u.s.}$	22
The Total Destructive Interference	
$E_{c.b.}$ with $E_{u.s.}$ (unfiltered)	25
Correction for Optical Component Scatter and	
Rayleigh Scatter	26
Determining $I_s(l)$	29
III. MAKING THE MEASUREMENTS	34
IV. ERRORS	37
Optical Component Errors	37
Laser Noise	37
Beam-Splitter Noise	37
Optical Flatness	38
Temperature Effects	39
Radiation Heating Effects	39
Ambient Temperature Variation Effects	39
Vibration	41
V. SIGNAL-TO-NOISE RATIOS	42

TABLE OF CONTENTS (CONTINUED)

Signal Received from Set-Up A	42
Signal Received from Set-Up B	43
Noise in Set-Up A	43
Noise in Set-Up B	44
Signal-To-Noise Ratios	44
VI. CONCLUSIONS	46
BIBLIOGRAPHY	48
APPENDIX	51

LIST OF FIGURES

<u>Figure</u>	<u>Page</u>
1.1 The Standard Nephelometer	3
1.2 Comparison between the scattering function (in absolute units) for ocean water (upper curve) and that for pure water (lower curve).	4
2.1 Michelson Interferometer	9
2.2 Divided wave packet when a path difference $2\Delta D$ exists between path No. 1 and path No. 2.	13
2.3 The "tails" left upon the recombination of two divided wave packets which have traveled unequal interferometric paths.	13
2.4 Resonant modes within an atomic emission line of 1 \AA width from a laser source.	17
2.5 Notation for the scattering of incident polarized light by a sphere	17
2.6 Radiation vector addition	20
2.7 Resultant vector due to the addition of the scattered and unscattered light	20
2.8 Apparatus for set-ups A and B	24
2.9 Polar plots of total scattered light intensity $[\frac{i_1+i_2}{2}]$ for single particles ($m=1.20$) illuminated by unpolarized light.	28
2.10 Vectorial relationship used to determine $\delta(\)$	33
3.1 Scattering element geometry	33

ERROR ANALYSIS OF INTERFEROMETRY IN MEASUREMENT OF FORWARD SCATTER IN SEAWATER

I. INTRODUCTION

The study presented here is an analysis of the feasibility and errors involved in measuring the volume scattering function $\beta(\theta)$ in the forward direction ($\theta=0^\circ$) using interferometric techniques. These techniques have not been previously employed in light scatter experiments primarily because of the lack of a suitable light source. With the advent of the laser source, with its extremely monochromatic and coherent characteristics, a study of the application of interferometry to scatter experiments is suggested as a means of extending our knowledge of the scattering properties of seawater. Such knowledge is highly important to oceanographers, not only in respect to their study of life in the sea, but also to their visual exploration of the oceans.

Due to the long time and high costs involved in constructing the interferometric experiment, it was suggested that a complete examination of the techniques and errors of scatter interferometry is in order. The results of this study are therefore intended as guidelines to the actual measurement of light scatter in seawater using interferometry.

The Volume Scattering Function

The volume scattering function $\beta(\theta)$ is defined by the equation

$$\beta(\theta) = \frac{J(\theta)}{HV} , \quad 1.1)$$

where $J(\theta)$ is the intensity of light scattered in the direction θ , and H is the intensity of light incident on the scattering volume V . Figure 1.1 shows the typical scatter geometry and the device with which it is usually measured. Such devices, called nephalometers, have been used in oceanographic studies for many years. A graph of $\beta(\theta)$ as a function of θ for a typical seawater is included in Figure 1.2. It should be noted that values of $\beta(\theta)$ for $10^\circ > \theta \geq 0^\circ$ and $170^\circ < \theta \leq 180^\circ$ are not shown and are not yet available.

Some of the first measurements of the volume scattering function $\beta(\theta)$ were made by Ramanathan (1923). His results indicated that the predominant scatterers are large in comparison with the wavelength of light. He also showed that the backscatter of light in seawater approaches that of light in fresh water. This indicates that the larger particles contribute relatively little backscattered light.

More recently, measurements of the volume scattering function $\beta(\theta)$ have been made by Sasaki (1960), Jerlov (1961), Tyler (1961), and Duntler (1963). However, such measurements are

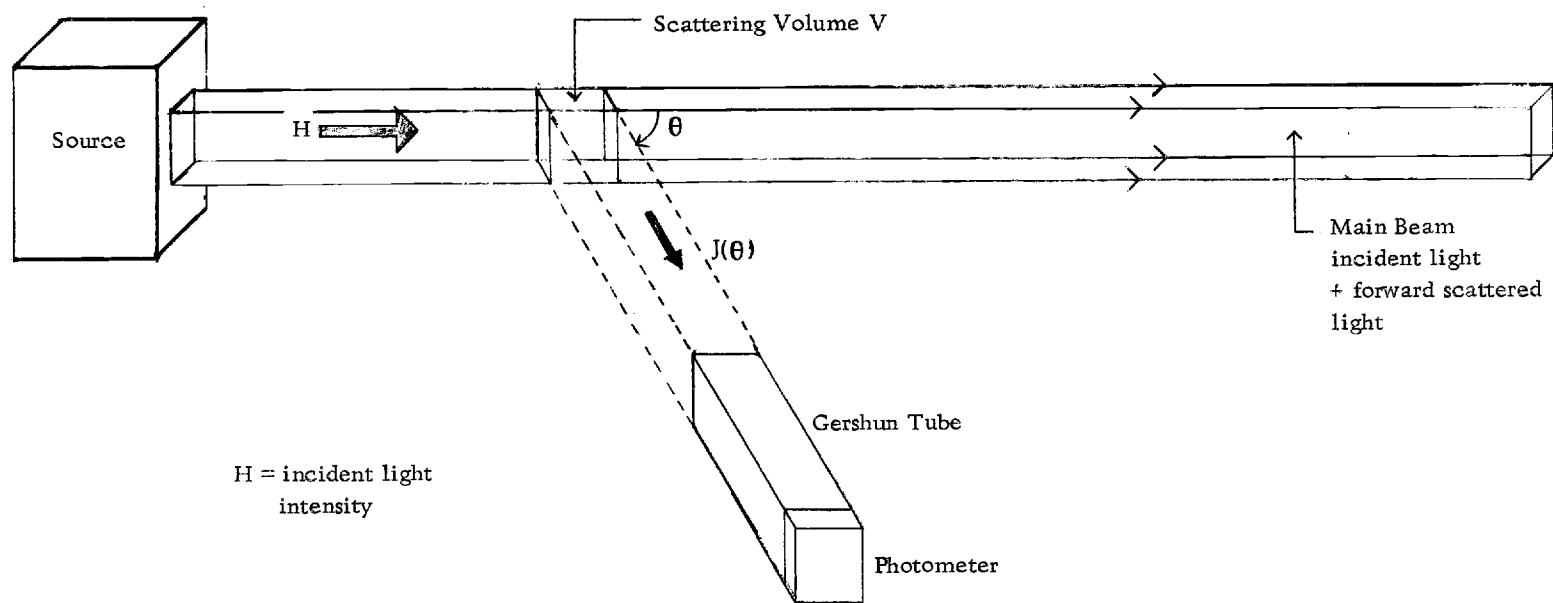


Figure 1.1: The Standard Nephelometer

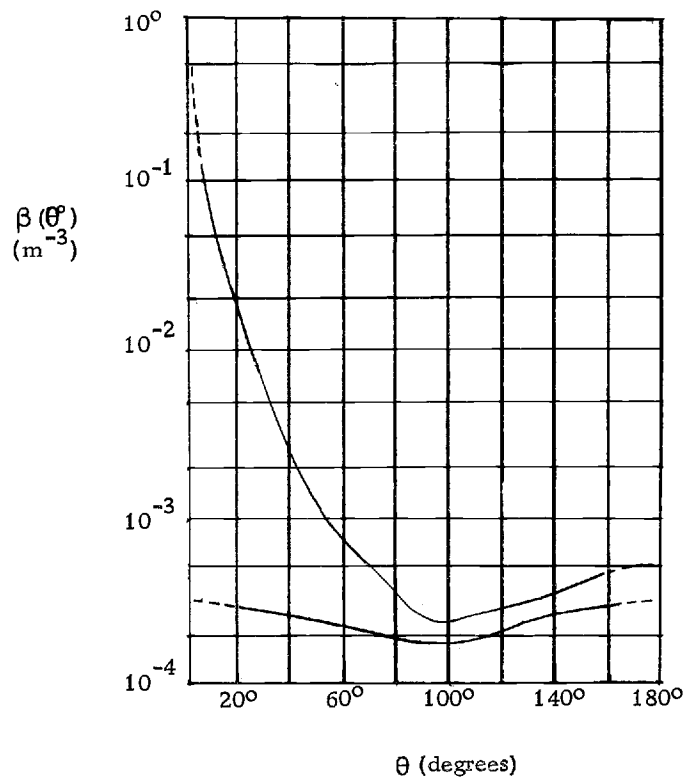


Figure 1.2: Comparison between the scattering function (in absolute units) for ocean water (upper curve) and that for pure water (lower curve). [from Jerlov (1961), page 15]

incomplete in that no measurement has been made of $\beta(0^\circ)$. It is seen from Figure 1.1 that when the photomultiplier tube is placed at an angle of 0° with the main beam, it reads both the unscattered incident light and the light scattered in the forward direction. Since the intensity of the light scattered in the forward direction is very small compared to that of the main beam, it is not distinguishable from the unscattered light by ordinary means.

For a given type of scatterer the total scattered light intensity is proportional to the total surface area of all of the scatterers in a given scattering volume if the diameter of each particle is greater than 2μ (Jerlov, 1955, Figure 1). For different types of scatterers the proportionality constant changes over a large range (Jerlov, 1955, Table 4).

By using $\beta(90^\circ)$ and the degree of polarization, p , at 90° , Ivanoff, Jerlov and Waterman (1961) were able to characterize various water types. They found that $\beta(90^\circ)$ is proportional to the total particle surface and largely independent of the particle form or dimensions; whereas p depends upon their shape and size, and is relatively independent of the total surface area.

Jenkins and Bowen (1946), and Atkins and Poole (1952) found that most of the incident light is scattered by particles whose diameters are of the same order or are larger than the wavelength of the incident light. They also found that most of the forward scattering

is due to many rather large, transparent particles with radii greater than 1μ . One of the most important reasons for measuring $\beta(\theta)$ at small values of θ is due to the relative importance of $\beta(0^\circ)$ in the computation of the total scattering coefficient.

Total Scattering Coefficient

The total scattering coefficient, b , is defined as

$$b = 2\pi \int_0^\pi \beta(\theta) \sin \theta d\theta. \quad 1.2)$$

The value of b is very much dependent on $\beta(\theta)$ from $\theta = 0^\circ$ to 10° , and these are the values for which β is least known. In fact $\beta(\theta)$ from $\theta = 0^\circ$ to $\theta = 5^\circ$ has never been measured. Jerlov (1961, page 11) says

. . . the integration (to find b) necessitates a rather delicate extrapolation of $\beta(\theta)$ from 10° to 0° and another from 165° to 180° which is readily made. The extension of the curve from 10° to 0° as suggested in Figure 6 [in this paper, Figure 1.2] is subject to uncertainty which may cause some error in b . It must be considered as an urgent task to furnish experimental evidence for scattering at low angles.

Spilhaus (1965) came the closest to finding $\beta(0^\circ)$; he used a narrow beam laser as a light source, and was able to make scattered light intensity measurements at an angle of less than 5° . His main interest was the identification of the predominant size of the scatterers of various water samples, and he devised various statistical

techniques to process his data.

In light of the above necessity of knowing $\beta(\theta)$ for small values of θ , a technique has been developed that proposes to measure $\beta(0^\circ)$ using an interferometer with a laser light source. This study examines the feasibility and inherent accuracy of the proposed techniques.

II. A METHOD PROPOSED TO FIND $\beta(0^\circ)$

It has been shown that the standard nephelometric method of measuring off-axis scattered light cannot be employed in the study of on-axis scatter. In order to ascertain the volume scattering coefficient for $\theta = 0^\circ$, an interferometric method is proposed.

Interferometry in Scatter Measurements

Interference due to the superposition of light waves has been observed for centuries. Thomas Young first demonstrated this phenomenon in 1802 and stated his "principle of superposition."

Certain basic conditions are necessary in order that maximum interference take place between two light waves:

- a) the two light waves must be colinear in path,
- b) the planes of oscillation of the two waves must be parallel,
and,
- c) the length of one of the waves must be completely overlapped by that of the other wave.

The interferometer has been a laboratory tool used mainly as a very precise length-measuring device. The Michelson interferometer (Figure 2.1) is one of the most accurate of the many different types of interferometers. Figure 2.8 is an example of a Michelson interferometer in which the use of various auxiliary

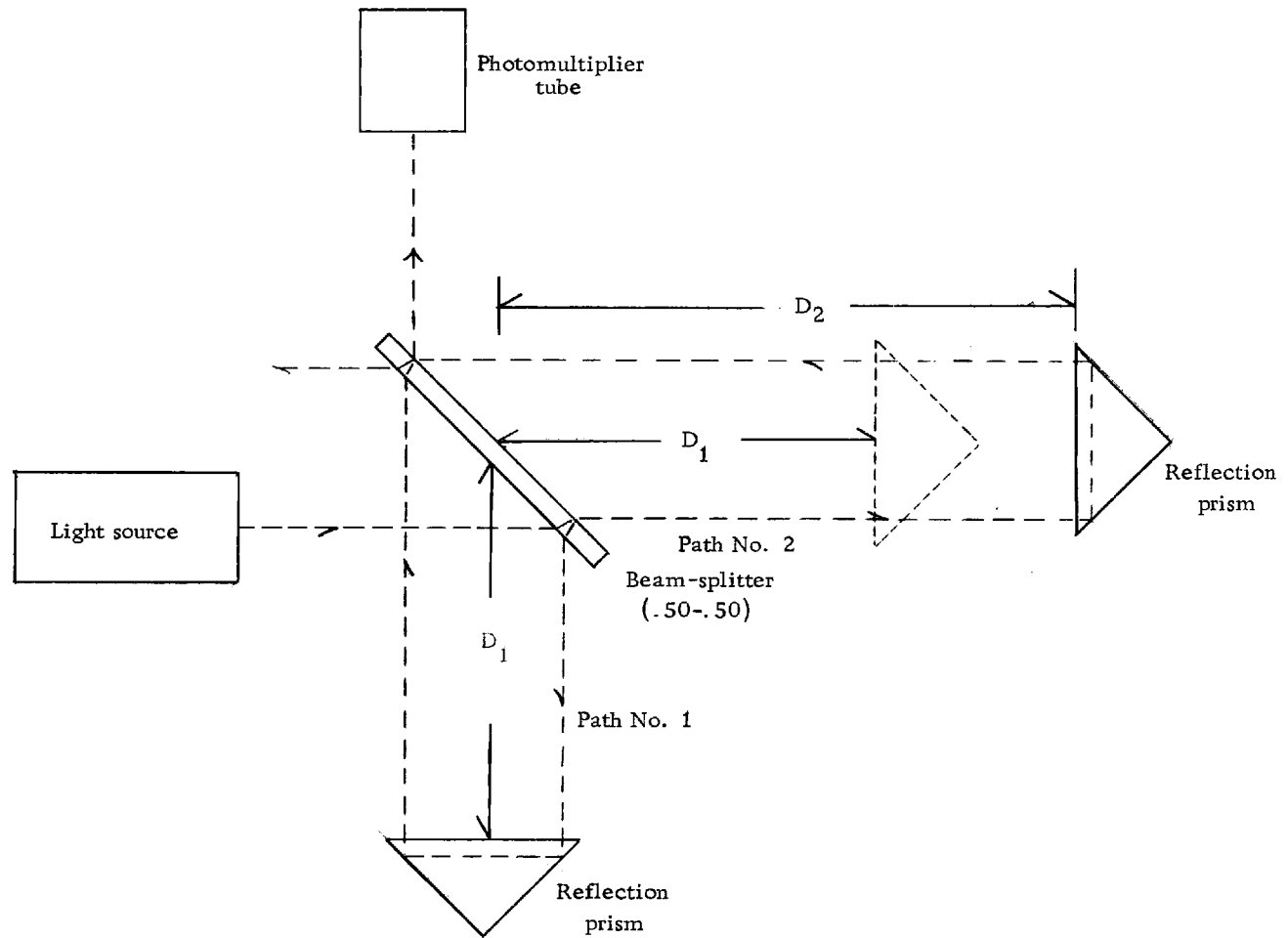


Figure 2.1: Michelson Interferometer

optical components allows two different interferometric schemes, set-up A and set-up B, to be used. The basic parts of this interferometer are the light source, beam-splitter, reflection prisms, and the photodetector. The other components are dealt with in later sections.

The design of the Michelson interferometer is based upon a division of the electromagnetic wave front into two parts and their subsequent recombination. It requires monochromatic, parallel, and spacially coherent radiation for optimum performance. In order to maintain a consistent interference pattern when the two optical paths of the divided wave front are unequal, an invariant phase and amplitude relationship must exist between successive wave packets. These conditions are at best only partially satisfied by conventional light sources.

Conventional Light Sources

Conventional light sources are at best only approximations to the interferometric source requirements stated in the previous section.

The Non-monochromaticity of Conventional Light Sources

Conventional sources, even with filters, are not monochromatic: a mercury vapor discharge lamp, for instance, has a

wavelength spread $\Delta\lambda$ of about 0.005 \AA about a center wavelength λ_0 of 5461 \AA (Jenkins and White, 1957). The mercury light is one of the most frequently used conventional sources for interferometry.

With a wavelength spread of 0.005 \AA , the wavelengths on the outer edges of this spread are 180° out of phase with each other after traveling only $546,100$ wavelengths or about ten inches. This causes them to destructively interfere with each other. As the waves travel even further from the source, waves having a $\Delta\lambda < 0.005 \text{ \AA}$ destructively interfere. So when this light is used in an interferometer, the bright fringes dim and lose contrast as the distance from the source increases. Thus, a constant dark-to-light fringe intensity ratio is not possible to maintain upon moving either of the interferometric arms.

If the optical paths of the two arms are not equal, even less fringe contrast results. In this case complete destructive interference becomes impossible. In general if the light is not monochromatic (assuming no wavelength spread) when the two divided wavefronts of a given wavelength recombine with a certain phase relationship, two divided wavefronts of a different wavelength will recombine with a phase relationship that is not the same.

The Incoherency of Conventional Light Sources

Conventional light sources are at best coherent for only very short

periods of time. They produce relatively short wave packets, and because of their general lack of spacial coherency, require that the interferometric optical path lengths be equal. It is easily seen from Figure 2.2 that if $2 \Delta D$ is greater than the length of the incident wave packet, no interference will take place. Even if $2 \Delta D$ is less than the length of the packet, interference takes place only between those portions of the two waves that overlap. Only if the two packets are very long and are very close to being completely overlapping can complete destructive interference take place. Since for a mercury vapor discharge lamp, these wave packets are only 20 inches long (Jenkins and White, 1957), the greater the distance ΔD , the smaller is the amount of recombination possible.

The "tails" left in Figure 2.3 combine with other packets, but the other wave packets in general are not in phase with that packet from which a given "tail" was divided, since conventional light sources are at best only partially coherent. The constant phase shifting between successive wave packets does not allow a proper recombination of these "tails" with respect to phase. So only if the optical paths No. 1 and No. 2 shown in Figure 2.2 are nearly equal, will a conventional source produce fairly usable fringes. In the measure of scatter as proposed herein, "fair" fringe contrast is not sufficient (Chapter V). Furthermore, with so many optical components in the interferometric paths (especially the seawater

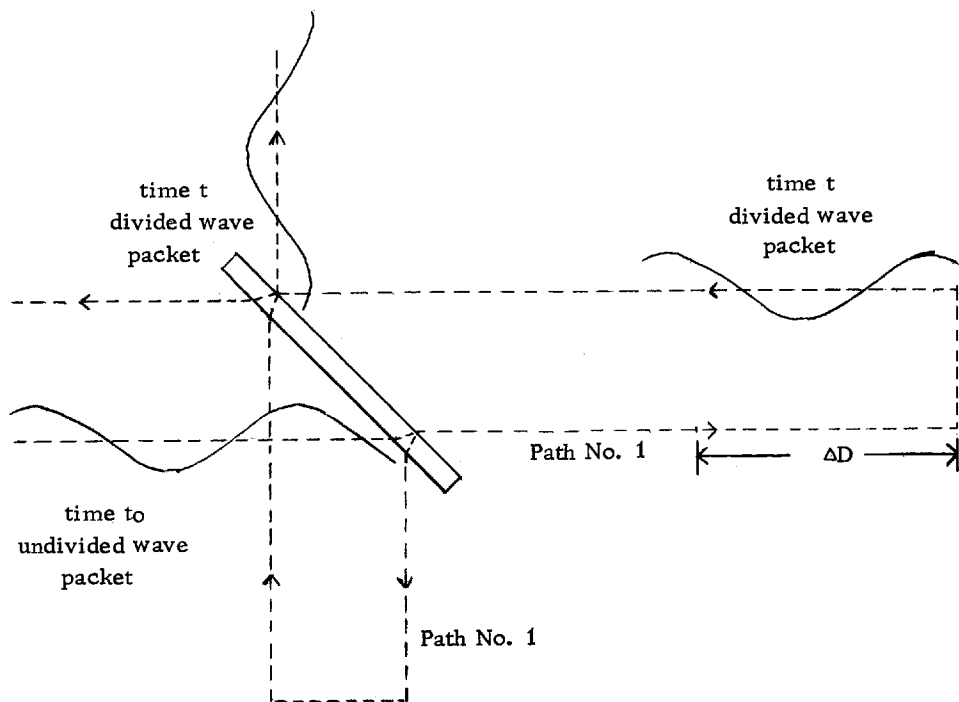


Figure 2. 2: Divided wave packet when a path difference $2\Delta D$ exists between path No. 1 and path No. 2.

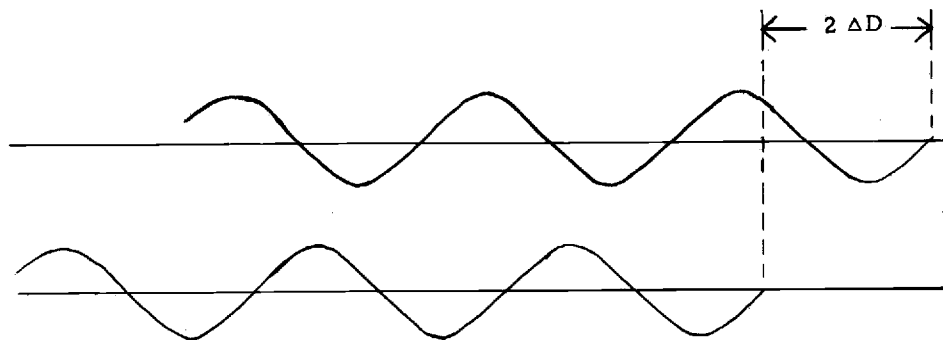


Figure 2. 3: The "tails" left upon the recombination of two divided wave packets which have traveled unequal interferometric paths.

itself) it becomes very unlikely that equal path lengths can be easily obtained.

If complete spacial coherency were attainable, the phases of all incoming wave packets would be the same. No matter what path difference, $2 \Delta D$, or wave packet length existed in this light, all of the wave packets in path No. 1 would be in phase. A similar situation would exist in path No. 2. Thus a constant phase relationship between different wave packets on the same optical path would be present. Infinite wave packet lengths would no longer be necessary to obtain "fine" interferometry as long as the source intensity remained constant and uniform.

The Non-parallelity of Conventional Light Sources

Conventional light sources radiate light in spherical patterns from each of a multitude of radiators, usually spread over a finite length or volume. Certainly if a small aperture were placed far enough away from the source, the light passing through it would approach parallelity. But, the geometrical attenuation of the source output energy would be prohibitive. A converging lens can be used fairly close to a point light source in order to intercept more energy than a distant aperture. If the light is placed at the focal length of the lens, the light is made parallel (assuming no lens aberrations). But a conventional source has a finite filament or discharge tube

length which again makes it a point source only if it is placed a long distance from the observer. If an aperture is used along with a lens, diffraction enters the picture, introducing interference patterns.

It is therefore necessary to use a light source superior to the conventional light sources in order that sharper, more contrasting interferometric fringes be produced.

Laser Sources

It was demonstrated in the preceding section that conventional light sources are less than ideal for interferometry. On the other hand, the latest continuous wave, uniphase, single mode lasers produce light that is monochromatic, uniphase, spacially coherent, and parallel. McNish (1964), Spectro-Physics Bulletins No. 's 1, 2, 3, and 4, Schawlow (1961), and Vogel and Dulberger (1961) present general pictures of laser theory. If more theoretical information is required by the reader, Kikuchi and Stroke (1965) is an excellent source.

The laser model suggested as applicable to this study is a helium-neon (He-Ne) gas laser with a power output of 100 micro-watts, a light wavelength of 6328.1983 \AA in air at 20° C (760 mm Hg), and an output frequency deviation from the center of the Ne^{20} emission line of $\pm 1 \text{ MC/day}$ (assuming an ambient temperature fluctuation of \pm one degree centigrade). This implies that the emitted wavelength

is $6328.1983 \pm 1.27 \times 10^{-5} \text{ \AA}$. This is obviously a very stable monochromatic beam. The previous specifications are available on the Model 119 Data Sheet of the Spectra-Physics Corp.

The divergence from parallelism of a good laser beam is less than 0.3 milliradians (0.0171°) if used with a collimating telescope. This is much better than could be expected from a conventional source.

Thus, for the finest accuracy in interferometry, a uniphase, continuous wave, single mode laser is suggested. The single mode (axial mode) is a very important property for an interferometric laser to have. Most lasers have several resonance modes within the Doppler width of a single emission line, as shown in Figure 2.4. Even if only two of the modes were present in the output spectrum of a laser, they would be 180° out of phase with each other after traveling only a distance of about 20 cm. This shows that a unimode laser is most desirable for interferometry, and mandatory if the optical path lengths are not nearly equal. The following section demonstrates theoretically why interferometry can be used to obtain forward scatter.

Mie Scattering Theory

Mie scattering theory is the most general scattering theory at present dealing with spherical scattering particles. The Rayleigh

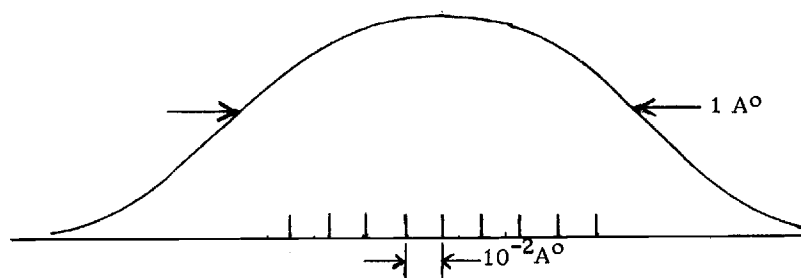


Figure 2. 4: Resonant modes within an atomic emission line of 1 Å width
 [from Kikuchi and Stroke (1965), Figure 2. 4] from a laser source

θ = angle between the scattering axis
 x and the observer o.

$E_{(i)}$ = incident light (polarized in the
 plane of the paper)

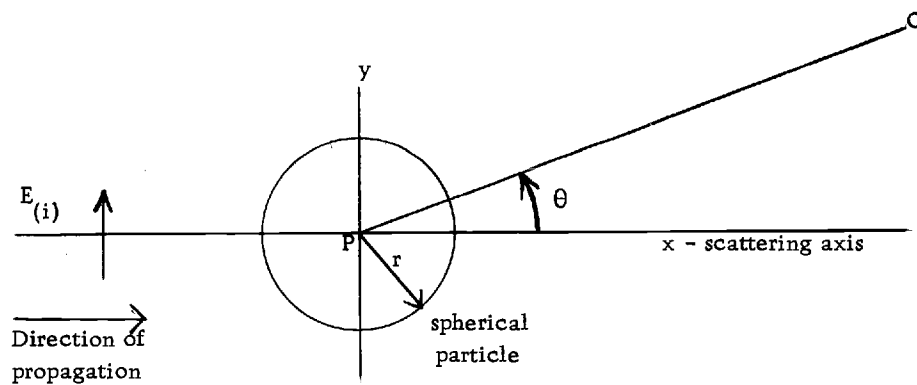


Figure 2. 5: Notation for the scattering of incident polarized light by a sphere

and geometrical scattering theories are simply limiting cases of Mie theory (i. e. when the particles are very small or large compared to the wavelength of the incident light). As was stated in Chapter 1, the greatest intensity of scattering by seawater is due to particles greater in diameter than 1μ . These particles are too large to be considered Rayleigh scatterers, whose radii must be less than one-tenth of the wavelength, and too small to be treated by diffraction theory. So, rigorous Mie theory has been applied to the seawater scattering of light.

Light having any degree of polarization may be described as being composed of the mutually perpendicular electromagnetic field vectors, $\bar{E}_{s(II)}$ and $\bar{E}_{s(I)}$. $\bar{E}_{s(II)}$ represents the vector sum of those components of the light field scattered by the particle, Figure 2.5, which lie in the plane formed by the scattering axis and the incident light vector \bar{E}_i . Call this the plane of polarization of the incident light. $\bar{E}_{s(I)}$ represents the sum of those components of the field of the scattered light which lie perpendicular to the plane of polarization of the incident light.

According to Mie theory, when incident plane-polarized light is scattered by spherical particles, it is depolarized to varying degrees, depending upon the size and shape of the particles, their index of refraction relative to the medium, and the angle of observation θ as shown in Figure 2.5. Spherical particles will theoretically

scatter light in the forward direction ($\theta = 0^\circ$) with a phase shift δ with respect to the phase of the incident light. The phase shift, δ , depends primarily on the size and index of refraction of the particles. Also, the parallel polarization component $\bar{E}_{s(\parallel)}$ exists, whereas the perpendicular polarization component $\bar{E}_{s(\perp)}$ does not exist when $\theta = 0^\circ$ (Van de Hulst, 1957). Non-spherical particles may also cause scatter having undergone a phase change $\delta \neq 0^\circ$. However, Mie theory does not pertain in the case of non-spherical scatterers. As a result, deviations from the above spherical particle scattering properties can be thought of as a qualitative measure of the non-sphericity of the scatterers; i.e., if $\bar{E}_{s(\perp)}$ exists, then non-spherical particles exist, and seawater scattering of light can no longer be arbitrarily assumed to behave like Mie scatter.

Distinguishing Various Types of Particles

Suppose that there are three types of particles which contribute most of the forward scattering. If these particles are of three different sizes, shapes, and substances, they will in general each exhibit scatter of a unique phase change δ_1 . If one adds the scattered light vectors, using only the parallel components, the identity of each type of scatter will be masked by the contributing scatter from the other kinds of particles (Figure 2.6).

The scattered light resulting from this arbitrary addition of

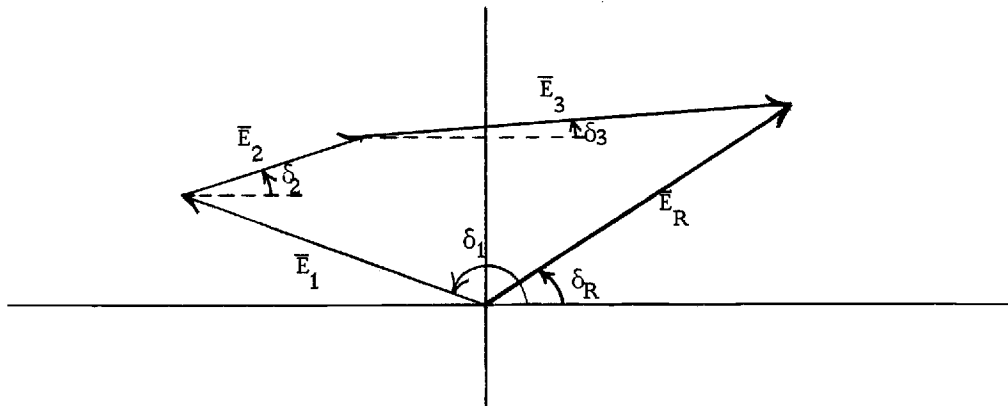


Figure 2.6: Radiation vector addition

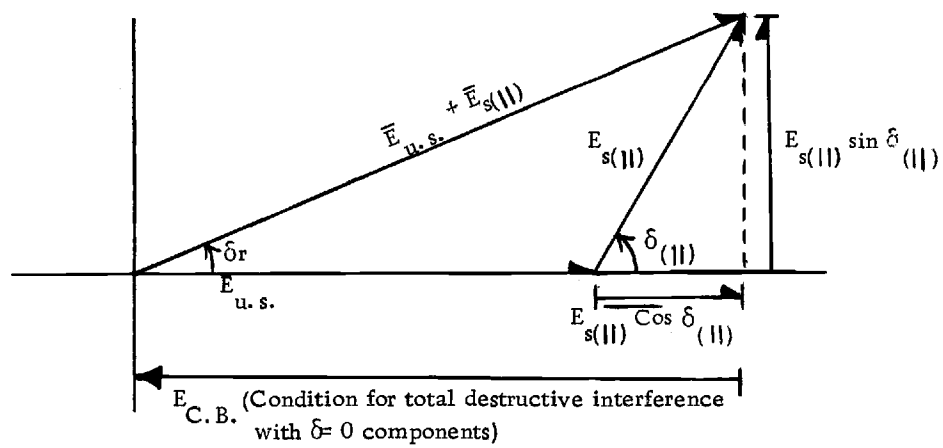


Figure 2.7: Resultant vector due to the addition of the scattered and unscattered light

waves can be thought of as having a resultant amplitude $|\bar{E}_R|$ with a phase change δ_R . \bar{E}_R is the only one of these vectors that will be instrumentally distinguishable. By filtering first the largest particles and then gradually decreasing the filter size, the specific characteristics of the scatter resulting from the absence of each size group can be determined. One can thus infer the contributions by any one size group to the total scatter.

Separating the Unscattered Light from
that Light Scattered Forward ($\theta=0^\circ$)

Let $\bar{E}_{u.s.}$ be that light vector which is unscattered, but which has traversed the scattering medium. Let $\bar{E}_{c.b.}$ be that light vector traversing path No. 1 in the interferometer. This light beam is referred to as the control beam (Figure 2.7).

The immediate problem is to separate the field contribution due to $\bar{E}_{s(||)}$ from that of $\bar{E}_{u.s.}$. In this case, $|\bar{E}_{u.s.}| \gg |\bar{E}_{s(||)}|$ and will tend to dominate.

From Figure 2.7 it is seen that if the control beam $\bar{E}_{c.b.}$ were adjusted in phase and intensity for total destructive interference with $\bar{E}_{u.s.}$, its phase would be 180° out of phase with $\bar{E}_{u.s.}$, and its amplitude would be equal to that of $\bar{E}_{u.s.}$. If the above destructive interference phase relationship exists and $|\bar{E}_{u.s.}|$ is not equal to $|\bar{E}_{c.b.}|$, call this destructive interference, but not total destructive

interference. The straightforward interferometric method only allows one to set the phase of the control beam vector 180° out of phase with the vector resultant $(\overline{E}_{u.s.} + \overline{E}_{s(||)})$. A roundabout method must be used in order to set the phase of $\overline{E}_{c.b.}$ 180° out of phase with $\overline{E}_{u.s.}$ alone.

Adjusting $\overline{E}_{c.b.}$ to Obtain Destructive
Interference with $\overline{E}_{u.s.}$

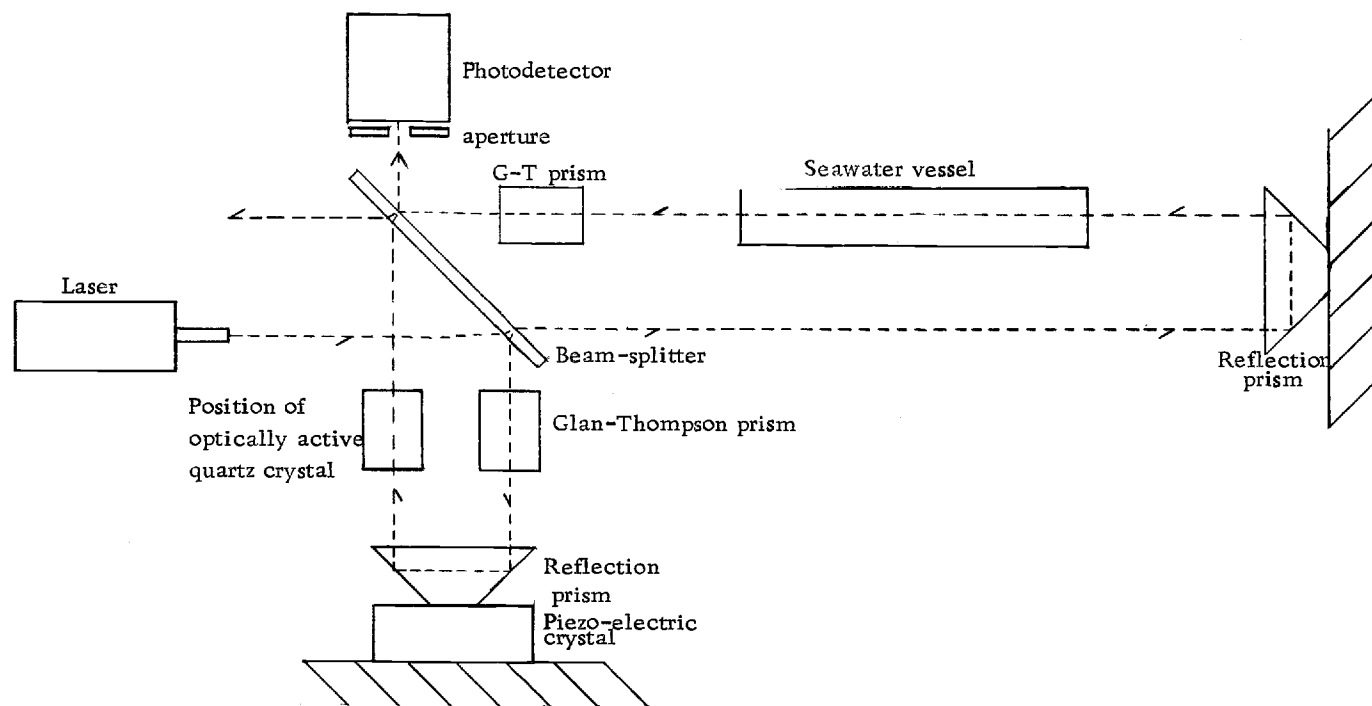
In order to set the phase of $\overline{E}_{c.b.}$ 180° out of phase with $\overline{E}_{u.s.}$, a volume of seawater is separated into two parts, one of which is very finely filtered. This removes the dominant scatterers, but the filtered seawater retains the index of refraction of the unfiltered part. According to Clark and James (1939), open ocean seawater may be Berkfeld filtered to a point at which light attenuation by this sample is nearly identical to that of double-distilled water. Thus, almost all particulate matter can be removed. Only unscattered and Rayleigh scattered light due to molecules and bacteria-sized particles are now present. Since particles of this size cause no phase change in the light scattered in the forward direction, and its scattered intensity is negligible with respect to the intensity of the unscattered beam,

$$[\overline{E}_{u.s.} + \overline{E}_{s(||)}]_{\text{filtered}} \doteq \overline{E}_{u.s.} (\text{filtered}) \quad 2.1)$$

In order to set the control beam so that it will be 180° out of phase with $\bar{E}_{u.s.}(\text{unfiltered})$, it is set 180° out of phase with $\bar{E}_{u.s.}(\text{filtered})$ since the phase of these two vectors are the same. This is accomplished by placing the filtered seawater in the seawater vessel in set-up A of Figure 2.8 and varying the current in the piezoelectric crystal. This crystal very minutely changes the length of the control beam path, altering the phase of $\bar{E}_{c.b.}$. The phase is adjusted until an intensity minimum, corresponding to destructive interference, is read on the photodetector. This process has placed $\bar{E}_{c.b.}$ 180° out of phase with $\bar{E}_{u.s.}(\text{unfiltered})$ and $\bar{E}_{u.s.}(\text{filtered})$.

In order to obtain the amplitude of $\bar{E}_{u.s.}(\text{filtered})$, it is necessary to now rotate the Glan-Thompson prism polarizer to attenuate the control beam to the point at which an absolute minimum is read on the photodetector. This fulfills the conditions necessary for total destructive interference. At this point $|\bar{E}_{u.s.}(\text{filtered})|$ equals $|\bar{E}_{c.b.}|$, and by blocking of the scattering path (No. 2) $|\bar{E}_{c.b.}|^2$ can be read directly on the photodetector.

When total destructive interference takes place for the filtered water, the intensity reading of the photodetector is due to Rayleigh and optical component scatter, called $I_{s(||)}'(\text{filtered})$. The removal of this noise quantity from the purely particulate scatter intensity is treated in a later section.



Set-up A: Quartz crystal removed

Set-up B: Quartz crystal present

Figure 2.8: Apparatus for set-ups A and B

The Total Destructive Interference

$\bar{E}_{c.b.}$ with $\bar{E}_{u.s. (unfiltered)}$

After replacing the filtered water with the unfiltered seawater, the control beam remains 180° out of phase with $\bar{E}_{u.s. (unfiltered)}$. To obtain total destructive interference of $\bar{E}_{u.s. (unfiltered)}$ with $\bar{E}_{c.b.}$, the amplitude of the control beam is adjusted so as to produce an absolute intensity minimum level on the photodetector. The intensity of the control beam itself is known at this point, for it can be measured on the photodetector by simply blocking off the scattering path (No. 2). Thus, for apparatus set-up A,

$$\bar{E}_{c.b.} = - \left[\bar{E}_{u.s.} + \overline{E_{s(||)} \cos \delta_{(||)}} \right]_{(unfiltered)},$$

as seen from Figure 2.7. In terms of intensity,

$$I_{c.b.} \propto \left| \bar{E}_{u.s.} + \overline{E_{s(||)} \cos \delta_{(||)}} \right|_{(unfiltered)}^2 = \left| \bar{E}_{c.b.} \right|^2 \quad 2.2)$$

The intensity minimum value on the photodetector when equation 2.2 is fulfilled is equal to that of $\left| \overline{E_{s(||)} \sin \delta_{(||)}} \right|_{r.m.s.}^2$.

There is no practical way of determining $\overline{E_{s(||)} \cos \delta_{(||)}}$ separately from $\bar{E}_{u.s. (unfiltered)}$, so since they are indistinguishable, $\overline{E_{s(||)} \cos \delta_{(||)}} + \bar{E}_{u.s. (unfiltered)}$ shall be called $\bar{E}_{u.s.}$, and $\overline{E_{s(||)} \sin \delta_{(||)}}$ shall be called $\bar{E}_{s(||)}$. Therefore $\delta_{s(||)} = 90^\circ$.

Equation 2.2 then becomes

$$I_{c.b.} = I_{u.s.} \quad 2.3)$$

$I_{u.s.}$, contains scattered intensity from Rayleigh particles in the unfiltered seawater and from optical components, as well as containing the scattered intensity from the particulate matter in the seawater. The following section proposes a method to separate the particulate-scattered light intensity of seawater from the Rayleigh and optical component scattered intensity.

Correction for Optical Component Scatter and Rayleigh Scatter

The primary reason for separating the seawater particulate scatter from Rayleigh and component scatter is for the comparison of the resultant data with Mie theory.

According to Burt (1955) the relative index of refraction m for the scatterers in seawater averages about 1.15. The relative index of refraction is the ratio of the index of refraction of the scatterer to that of the medium (seawater). Jerlov (1961) estimated from his curves of the volume scattering angle θ that the average particle size of offshore seawater is around 10μ . He found by comparing his own nephelometric scattering curves to those of various theoretically computed Mie scattering curves, that his curves most closely paralleled the Mie curves for $m = 1.20$ and $r = 3 \times 10^{-6}$ meters (Mie curves were worked out by Ashley and Cobb (1958).

Since light scattered by water molecules and any particles

small enough to pass through a Berkfeld No. 5 filter, is scattered essentially by Rayleigh scatterers ($\text{radii} < 0.1\lambda$), it is negligible compared to that of seawater particulate scatter in the forward direction. As a particle increases in size, its scatter becomes more intense in a predominantly forward direction. Figure 2.9 illustrates the importance of particle size in the scattering of light. The following three paragraphs of quotation help to define the quantities found in Figure 2.9 as stated by Ashley and Cobb (1958):

The intensity functions, i_1 and i_2 , which are proportional to the intensities of the two incoherent, plane-polarized components of light scattered by a single illuminated particle, were evaluated for angles of observation from 0° to 170° in ten-degree intervals, and from 171° to 180° in one degree intervals.

When the particle is illuminated by plane-polarized light of unit intensity per unit cross-sectional beam area, $(\lambda^2/4\pi^2)i_1$ is the intensity of the scattered component whose electric vector is perpendicular to the electric vector of the incident beam; $(\lambda^2/4\pi^2)i_2$ is the intensity of the scattered component whose electric vector is parallel to the plane of the electric vector of the incident beam and its direction of propagation.

When the particle is illuminated by unpolarized light of unit intensity per unit beam cross-sectional area, $(\lambda^2/8\pi^2)i_1$ is the intensity (per unit solid angle) of the scattered component whose electric vector is perpendicular to the plane of observations; $(\lambda^2/8\pi^2)i_2$ is the intensity of the scattered component whose electric vector is parallel to the plane of observation.

The definitions of i_1 and i_2 follow that of Mie theory and can be found in Born and Wolfe (1959) or Van de Hulst (1957). In the forward direction $i_2 = 0$, so $i_1/2 = (i_1 + i_2)/2$. For angles other than 0° Figure

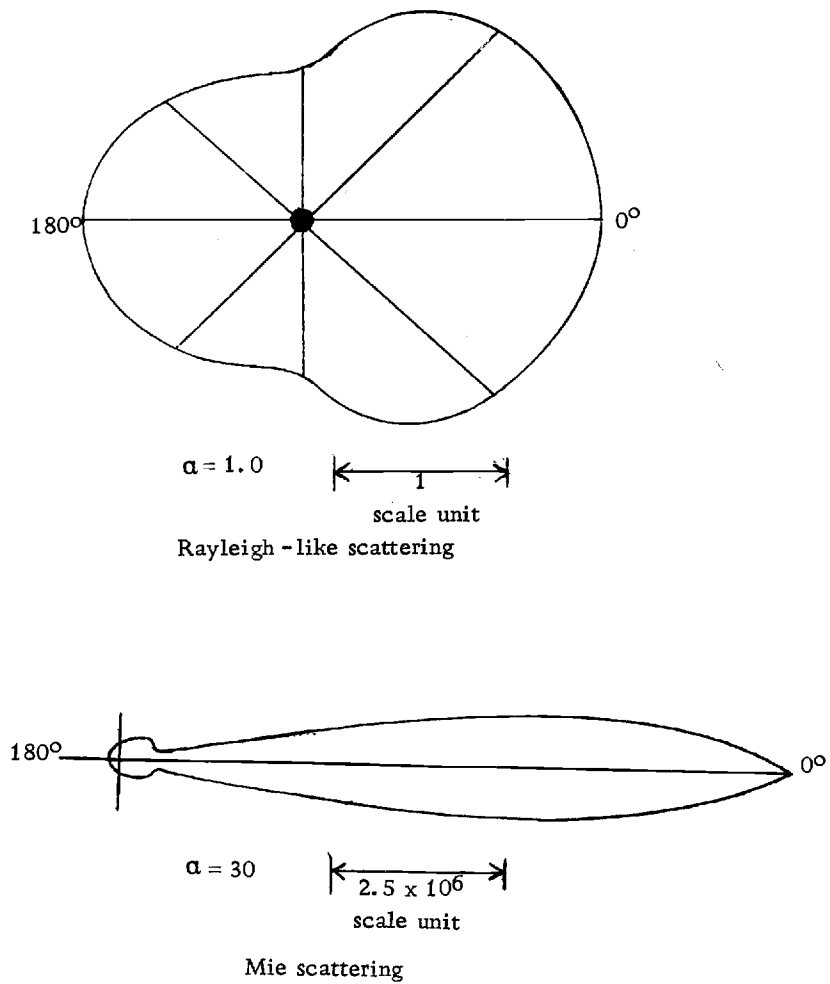


Figure 2.9: Polar plots of total scattered light intensity, $\left[\frac{i_1 + i_2}{2} \right]$, for single particles ($m=1.20$) illuminated by unpolarized light [from Ashley and Cobb, 1958, page 267].

2.9 represents an average of i_1 and i_2 .

From Figure 2.9 it is seen that not only does a larger particle intercept and scatter a much larger amount of light than does a Rayleigh-like scatterer, but the resulting scattered light intensity is very predominantly in the forward direction as compared to the nearly uniform distribution of intensity with respect to scattering angle of the Rayleigh scatterer.

Nevertheless, if $I_{s(||)}'(\text{filtered})$ is subtracted from $I_{s(||)}'(\text{unfiltered})$ the effects of Rayleigh and optical component scatter will be subtracted out, leaving only the intensity of the light scattered by the particulate matter in seawater.

$$I_{s(||)}'(\text{unfiltered}) - I_{s(||)}'(\text{filtered}) = \begin{array}{l} \text{Intensity in the incident} \\ \text{plane of polarization due} \\ \text{only to the scattering of} \\ \text{light by seawater parti-} \\ \text{cles} \end{array} \quad 2.4$$

A different technique is necessary in order to determine the perpendicular polarization component $\bar{E}_{s(\perp)}$, if it exists.

Determining $I_{s(\perp)}$

In apparatus set-up A, the control beam is used to destructively interfere with $\bar{E}_{u.s.}$. In apparatus set-up B, the unscattered vector $\bar{E}_{u.s.}$ is blocked by the polarizer, so that the function of the control beam is primarily that of determining the phase shift $\delta_{(\perp)}$ of the scattered light. $\bar{E}_{u.s.}$ is blocked by rotating the polarizer in the

scattering path until its plane of transmission is perpendicular to the plane of polarization of $\bar{E}_{u.s.}$. This allows the transmission through the polarizer of only $\bar{E}_{s(\perp)}$. In this case, the optical component scatter, laser noise, as well as the Rayleigh scatter are blocked by the polarizer. So, only unfiltered seawater need be used in the seawater vessel.

In order to determine the phase shift $\delta_{(\perp)}$ of $\bar{E}_{s(\perp)}$, the phase of the control beam must be adjusted 180° out of phase with the incident beam. To do this, the scattering path polarizer is rotated so as to allow $\bar{E}_{u.s.}$ to be transmitted. Then, by adjusting the piezo-electric crystal, the phase of $\bar{E}_{c.b.}$ is shifted until an intensity minimum appears on the photodetector. This satisfies the conditions necessary for destructive interference to take place.

The problem now is to rotate the plane of polarization of $\bar{E}_{c.b.}$ by 90° in order that it can interfere with $\bar{E}_{s(\perp)}$ (condition b, chapter II). The placement of a 90° polarization plane rotator (optically active quartz) in the control beam accomplishes the necessary rotation. Let the electromagnetic field vector $\bar{E}_{c.b.(\perp)}$ denote the light field vector of the rotated control beam. Set-up B of Figure 2, 8 shows the proposed placement of the above rotator. This rotator must be designed so as to induce no phase shift on the control beam upon insertion in it. This can be accomplished by building up an optical coating on one of the crystal ends to the point at which the

the light traveling through this crystal departs from it with the same phase as it would have had if the crystal had never been inserted into the beam. Finally, the scattering path polarizer is returned to its perpendicular orientation.

$\overline{E}_{c.b.(\perp)}$ is now 180° out of phase with $\overline{E}_{u.s.}$ and its plane of polarization is perpendicular to that of $\overline{E}_{u.s.}$. By adjusting the phase of $\overline{E}_{c.b.(\perp)}$ so as to produce a minimum on the photodetector, it will have undergone a phase shift of $\delta_{(\perp)}$ in reaching a state of destructive interference (Figure 2.10). The phase shift, $\delta_{(\perp)}$, can be detected by calibrating the piezo-electric crystal. This leaves only $|\overline{E}_{s(\perp)}|$ to be determined.

The amplitude of $\overline{E}_{s(\perp)}$ can be most easily determined by simply blocking off the light of the control beam from the detector. The intensity occurring on the detector is due to $|\overline{E}_{s(\perp)}|^2$. This intensity is called $I_{s(\perp)}$.

Knowing $I_{s(\parallel)} + I_{s(\perp)}$,

$$I_{s(\parallel)} + I_{s(\perp)} = \text{Total forward scatter } (\theta = 0^\circ). \quad 2.5)$$

Since δ is more a function of m and particle thickness than it is of particle shape, it is expected that $\delta_{(\parallel)} = \delta_{(\perp)}$, since they are both phase change averages.

As was mentioned earlier, if $I_{s(\perp)}$ is too small to measure, this is an indication that the scatterers are sphere-like in their

statistical scattering properties at least in this respect. If $I_{s(\perp)}$ is measurable, at least some of the particles can no longer be considered sphere-like or Mie scatterers.

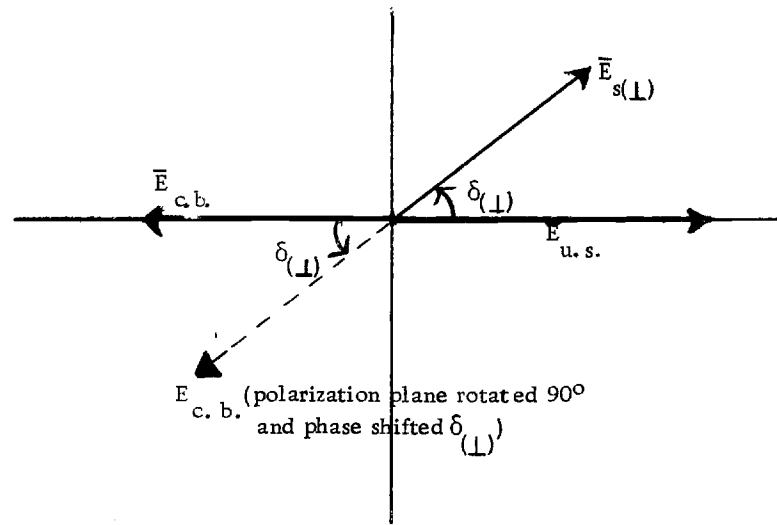


Figure 2.10: Vectorial relationship used to determine $\delta_{(\perp)}$

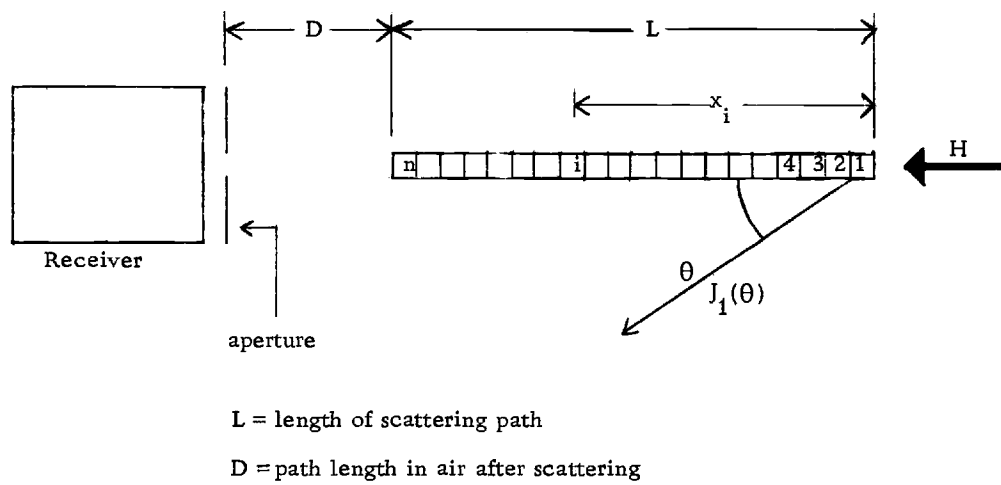


Figure 3.1: Scattering element geometry

III. MAKING THE MEASUREMENTS

The scattered light intensity at some angle θ is called $J(\theta)$.

If this light is scattered from a large scattering volume V , this volume must be subdivided into n subvolumes or scattering elements in order to define each of the angles θ_i formed by the scattering axis and the line between the i^{th} subvolume and the observer. Each of the different subelements receive different amounts of incident light intensity H_i , depending upon how much light attenuation takes place at varying places along the scattering path. Referring to Figure 3.1,

$$J_i(\theta) = H_i V_i \beta(\theta), \quad 3.1)$$

where

$J_i(\theta)$ = intensity of scattered light in the direction θ from element i , measured in microwatts/steradian;

$H_i(\theta)$ = laser beam intensity incident on the sample volume V , in microwatts/cm²;

V_i = volume of scattering element No. i , in cm³; and

$\beta(\theta)$ = volume scattering coefficient in cm⁻¹ steradian⁻¹. Then

the intensity scattered at $\theta = 0^\circ$ from scattering element No. 1 is

$$J_1(0^\circ) = H_1 V_1 \beta(0^\circ).$$

There is a certain amount of attenuation due to traveling in water from volume No. 1 to the receiver. So, the intensity of light

actually reaching the receiver due to scatter from volume element

No. 1 is

$$1/2 J_1(0^\circ) = 1/2 H_1 V_1 \beta(0^\circ) e^{-\alpha L} = I_1(0^\circ), \quad 3.3)$$

where H_1 = incident unscattered beam flux incident on volume element No. 1,

α = total attenuation coefficient per unit length, as measured by the attenuation necessary to impose on the control beam in order to receive a minimum receiver output, in cm^{-1} , assuming only single-particle scattering. The "1/2" comes from the reflection off the beam-splitter.

The intensity at the receiver due to light scattered from the x_i element is

$$1/2 J_i(0^\circ) = 1/2 H_i V_i \beta(0^\circ) e^{-\alpha(L-x_i)} = I_i(0^\circ), \quad 3.4)$$

where $H_i = H_1 e^{-\alpha x_i}$

Thus, the total intensity due to forward scattered light arriving at the receiver is then

$$1/2 J_{\text{total}}(0^\circ) = \frac{1}{2} \sum_{i=1}^n J_i(0^\circ) = 1/2 \sum_{i=1}^n H_1 V_i \beta(0^\circ) e^{-\alpha L} \quad 3.5)$$

$$= I_{\text{total}}(0^\circ) = \frac{1}{2} H_1 \beta(0^\circ) e^{-\alpha L} \sum_{i=1}^n V_i \quad 3.6)$$

$$\text{But } V_1 = V_2 = \dots = V_n \quad \sum_{i=1}^n V_i = n \cdot V_1$$

$$\beta(0^\circ) = \frac{J_{\text{total}}(0^\circ)}{n H_1 V_1 e^{-\alpha L}} = \frac{2 I_{\text{total}}(0^\circ)}{n H_1 V_1 e^{-\alpha L}} \quad 3.7)$$

In this case $I_{\text{total}}(0^\circ) = I_{s(\parallel)} + I_{s(\perp)}$, so

$$\beta(0^\circ) = \frac{2(I_{s(\parallel)} + I_{s(\perp)})}{n H_1 V_1 e^{-\alpha L}} \quad 3.8)$$

Then, $\beta(0^\circ)$ is obtainable using the interferometric method discussed herein, assuming the noise in the system is low enough to allow an unobscured signal to be detected.

IV. ERRORS

The errors in this system can be categorized as being due to optical components, temperature effects, and vibration.

Optical Component Errors

The dominating optical component errors are caused by the laser, the beam-splitter, and the optical flatness of the component surfaces.

Laser Noise

The noise of the laser proposed for this interferometry experiment is less than $0.1\% I_0$ and is caused primarily by amplitude variations in the intensity output. This quantity was measured using interferometry, so it also includes an optical vibration factor. By maintaining nearly equal interferometric optical lengths, a large fraction of this error could be reduced. In this case, though, the noise is assumed to be 0.1% (personal communication with John Bacevic).

Beam-Splitter Noise

The front surface (glass) of the beam splitter reflects $0.5\% I_0$ even though it is coated (personal communication with L. S. Howerton),

and this light is out of phase and linearly displaced from that light reflected from the back surface of the mirror. This effect is most apparent in the control beam, but a similar offset, out of phase reflection takes place in the scattering path. Considering the various attenuations along the path, the resultant beam-splitter reflection noise is less than $0.3\% I_o$.

Optical Flatness

If a component is listed as having an optical flatness of $1/20 \lambda$ over the central one-half inch, this means that any portion of the surface could transmit light that is out of phase by $1/20 \lambda$ with that of some other portion. Assume that a linear relationship exists in terms of phase from one point to the next; otherwise distortion would be apparent. Therefore, assuming a linear relationship at least in fairly small regions, one portion may be $1/20 \lambda$ out of flatness with another over a linear distance of say one-half inch. Thus

$$1/20 \lambda \left(\frac{\text{width of beam}}{1/2 \text{ inch} = 1.3 \text{ cm}} \right) = \frac{1}{20} \lambda \left(\frac{3 \text{ mm}}{13 \text{ mm}} \right), \quad 4.1)$$

$$\left. \begin{array}{l} \text{or the error} \\ \text{in phase of} \\ \text{wavefront} \end{array} \right\} = \pm 4^\circ$$

Then an error in n components of $\pm 4^\circ$ each is $\pm \sqrt{n} (4^\circ)$. In the scattering beam, $n = 6$. In the control beam, $n = 5$. Therefore, the total error in the coherence of the wavefront is $\pm \frac{1}{2} \sqrt{5+6} (4^\circ)$ or

$\pm \sqrt{11/2}(4^\circ)$ or $\pm 6.6^\circ$. This manifests itself in an amplitude intensity error of $\pm .0036 I_0$.

Temperature Effects

Radiation Heating Effects

If the water in the scattering path absorbed as much as 1 microwatt of power (this figure is exorbitant) and assuming that there are only ten grams of seawater in the vessel, its temperature would rise by about $2.4 \times 10^{-6}^\circ \text{C}$ every 100 seconds, assuming no heat losses. This temperature increase is negligible. Thus, no operating time limit need be adhered to with respect to radiant heating from the laser.

Ambient Temperature Variation Effects

It is of extreme importance to maintain the filtered and unfiltered seawater at exactly the same temperature, for a small difference in temperature will introduce a large phase shift during the exchange of seawater samples. Sufficient temperature control can be accomplished by using a water bath accurate to $\pm 0.01^\circ \text{C}$. Even this small a fluctuation in temperature induces a variation in the index of refraction of seawater of about 9×10^{-7} assuming the temperature to vary around 20°C . Such a variation in the index of

refraction will cause a change of phase of about $\pm 4.2^\circ$ if the water vessel is only 1 cm long.

If the optical lengths in the air, crystals, and glass components are the same for each path, a small ambient temperature change will affect both paths identically assuming that the temperature change is the same for each path. In this way no phase change is induced between the two optical paths due to temperature effects. The two optical paths can be maintained at equal temperatures by locating the interferometer in an enclosed box with a small fan inside. The fan will maintain a spacially uniform temperature and humidity at all places within the box, even though these have time variations. Thus, if the room temperature fluctuates by only a degree or two, temperature errors will change the phase of the light passing through the unfiltered versus the filtered seawater by at most $\pm 5^\circ$, since there will be negligible phase variations due to temperature effects on the optical components.

To illustrate the need for equal lengths of quartz, glass, and air in each of the optical paths, let us assume that there is a quartz crystal of 1 cm. length in only one of the paths. According to the International Critical Tables (1934), the index of refraction for quartz is 1.542819 at 15°C . This number changes by -5.49×10^{-6} per degree centigrade in this range of temperature. Therefore, in traveling through a 1 cm. length of quartz, a -27.7° phase change takes

place due to a temperature increase of 1°C . But there is also an expansion of the quartz crystal. If $\Delta T = 1^{\circ}\text{C}$, then the change in length is about 5×10^{-5} cm. or about 1.54 wavelengths. The combination of both temperature effects causes a phase change due to a 1°C rise in temperature of 529° or about 1.47 wavelengths. This same type of analysis holds true for the other optical components. So, equalizing the optical lengths of each type of component is the only way to minimize phase changes due to changes in the ambient temperature.

Vibration

It is possible to reduce vibration to a level negligible with respect to laser noise (personal communication with John Bacevic, of Spectra-Physics). Each of the major noise and error factors have been dealt with individually, but they will vary in their cumulative effect depending upon the apparatus set-up being used. The basic feasibility test of an experiment is the comparison of the signal received with the cumulative noise and errors induced by the equipment.

V. SIGNAL-TO-NOISE RATIOS

In order to predict whether or not a set of measurements will be meaningful, the strength of the signal must be dominant over that of the combined noise factors.

Signal Received from Set-Up A

A certain amount of the incident light will be lost to component attenuation, but this will be less than 0.3% for each optical element. If I_o is the intensity of the laser beam, about 1/2 of it is lost by reflection off the beam-splitter. Therefore, the signal reaching the seawater will be at least $0.49 I_o$.

$$\text{According to Jerlov (1961), } \beta(0^\circ) > .1 < \frac{J(0^\circ)}{HV}, \quad 5.1)$$

$$\text{or } J(0^\circ) > 0.1 HV, \quad 5.2)$$

$$\text{where } H = 0.49 I_o, \text{ and } V = \pi (.0035)^2 (0.01) m^3.$$

$$\text{Then } J > (.1)(.49 I_o)(.0035)^2 (\pi)(0.01). \quad 5.3)$$

$$> (.49 I_o)(4.0 \times 10^{-8})$$

$$J > 2.0 \times 10^{-8} I_o.$$

But more than one-half of J is lost going through the polarizer and the beam-splitter.

$$I_{s(||)} \sin \delta_{(||)} > 1.0 \times 10^{-8} I_o \frac{\mu \text{watts}}{\text{cm}^2}. \quad 5.4)$$

If $\delta_{(||)} = 90^\circ$, $I_{s(||)} > 1.0 \times 10^{-8} I_o$. But as will be seen in a later section, even this signal is not intense enough with respect to noise, let alone one having a $\sin \delta_{(||)} < 1$.

Signal Received from Set-Up B

The signal received from set-up B, $I_{s(\perp)}$, is theoretically zero. If it does actually exist, its intensity must be greater than the intensity of the noise in order to be distinguishable. In the section on Signal-to-Noise Ratios the value above which $I_{s(\perp)}$ as a signal can be recognized is derived. This minimum intensity below which a signal for $I_{s(\perp)}$ cannot be separated from the experimental noise in set-up B is called the threshold intensity of $I_{s(\perp)}$. If $I_{s(\perp)}$ does not exceed its threshold intensity, it can only be assumed to be negligible.

Noise in Set-Up A

The maximum noise arriving at the receiver will be as follows for set-up A:

$$\begin{aligned}
 I_{\text{noise A}} &\triangleq \frac{1}{2} (.001 I_o) + \frac{1}{4} (.005 I_o) + \frac{1}{4} (.0036 I_o) & 5.7) \\
 &\quad \text{Laser noise} \quad \text{control beam} \quad \text{flatness} \\
 &\quad \quad \quad \text{beam-splitter} \quad \text{noise} \\
 &\quad \quad \quad \text{noise} \\
 &+ \frac{1}{4} (.005 I_o) = 0.0039 I_o \text{ or } 0.004 I_o \\
 &\quad \text{scatter path} \\
 &\quad \text{beam-splitter} \\
 &\quad \text{noise}
 \end{aligned}$$

where I_o is the intensity of the laser output in $\mu \text{ watts/cm}^2$.

Noise in Set-Up B

The maximum noise arriving at the receiver will be as follows for set-up B:

$$I_{\text{noise B}} = 1/2 (.001 I_o + .005 I_o) K \quad 5.8)$$

laser and
beam-splitter
noise

where K is the attenuation due to the polarizer.

$$I_{\text{noise B}} < 0.003 K I_o \quad 5.9)$$

$$\text{but } K < I_s(\parallel) \sin \delta_{(\parallel)} = 1.0 \times 10^{-8}. \quad 5.10)$$

$$\text{So } I_{\text{noise B}} \doteq (3.0 \times 10^{-3})(1.0 \times 10^{-8}) I_o \quad 5.11)$$

$$I_{\text{noise B}} \doteq 3.0 \times 10^{-11} I_o \mu \text{ watts/cm}^2. \quad 5.12)$$

Signal-To-Noise Ratios

It is clear from the results of the preceding sections that set-up A will not allow a strong enough signal with respect to the optical noise. The signal-to-noise ratio for set-up A is from equation (5.4) and equation (5.7)

$$\frac{S_A}{N_A} > \frac{5.0 \times 10^{-9} I_o}{4.0 \times 10^{-3} I_o} = 1.25 \times 10^{-6} \quad 5.13)$$

This means that the signal-to-noise ratio for $I_{s(||)}$ is less than 1.25×10^{-6} , a value much too small to be useful.

For set-up B, the signal-to noise ratio is much more favorable. A signal as small as $3.0 \times 10^{-11} I_o$ is detectable, assuming a generous signal-to-noise ratio of 1. In order that $\delta_{(\perp)}$ be determined, it must be quite a bit larger than $\pm 5^\circ$ in order to be considered detectable, since the error in phase detection is about $\pm 5^\circ$. By taking several different readings of $\delta_{(\perp)}$, the most probable error involved can be reduced to a value much smaller than $\pm 5^\circ$. For example, if 30° is the average $\delta_{(\perp)}$ found from five different readings, then the most probable error calculated from the deviations from the mean will be much smaller than $\pm 5^\circ$. This is assuming that any given deviation from the mean is less than or equal to $\pm 5^\circ$.

VI. CONCLUSIONS

Several conclusions may be drawn from these studies. It became apparent almost immediately that a laser source of light for the interferometer is needed. As it turned out, even the laser selected as being best suited to this interferometric problem has too much noise for one aspect of the study.

It was found that particular contributions to the total scatter by any one size group of particles can be determined. This is assuming that all measurements of the scattered light are detectable.

An important result is that the separation of the forward scattered light from the unscattered light is possible by using interferometry, even though at present the equipment necessary to measure such scatter produces too much noise. Going farther, that component of the scattered field vector $\bar{E}_{s(||)}$ having no phase shift is considered a part of $\bar{E}_{u.s.}$ since it is found to be indistinguishable from $\bar{E}_{u.s.}$. As a result only the component having a 90° phase shift, $\bar{E}_{s(||)'}'$, is considered to be scattered light in the incident plane of polarization. This means that the intensity of the light scattered in the forward direction by seawater particles is equal to $I_{s(||)'} + I_{s(\perp)}$.

In developing a workable expression for $\beta(0^\circ)$ for a seawater vessel of length L , being broken up into n subvolumes,

$2(I_{s(||)} + I_{s(\perp)})/n H_1 V_1 e^{-\alpha L}$ was derived. Due to the length of this vessel and the number of optical components involved, it was determined that temperature must be carefully controlled.

Finally, the detection of $I_{s(||)}$ was found to be impossible using what is considered to be the best currently available laser source for this interferometric method. Excessive noise with respect to the expected signal is the quantity responsible for this failure. In contrast, a signal for $I_{s(\perp)}$ as small as $3.0 \times 10^{-11} I_o$ is detectable in set-up B. But, if a value for $I_{s(\perp)}$ is found to exist, then Mie scattering theory cannot be applied directly to seawater scattering of light.

Since $\beta(0^\circ)$ is not attainable using the interferometric apparatus described herein, an alternate method is described in the appendix.

It is worth mentioning that the volume attenuation coefficient, α , for seawater can be determined directly by using the previously mentioned apparatus. The laser, scattering vessel, and photodetector allow α to be measured directly.

BIBLIOGRAPHY

- Ashley, L. E. and C. M. Cobb. 1958. Single particle scattering functions for latex spheres in water. *Journal of the Optical Society of America* 48:261-268.
- Atkins, W. R. G. and H. H. Poole. 1952. An experimental study of the scattering of light by natural waters. *Proceedings of the Royal Society, ser. B*, 140:32-338.
- Bacevic, John. 1966. Company representative, Spectra-Physics, Mountain View, Calif. Personal communication. July, 1966.
- Bloom, A. L. 1964. Properties of laser resonators giving uniphase wave fronts. *Spectra-Physics Laser Technical Bulletin*, no. 2: 1-5.
- Bloom, A. L. 1965. Noise in lasers and laser detectors. *Spectra-Physics Laser Technical Bulletin*, no. 4:1-10.
- Born, Max and Emil Wolfe. 1964. *Principles of optics*. 2d rev. ed. Oxford, Pergamon Press. 808 p.
- Burt, Wayne V. 1955. Interpretation of spectro-photometer readings on Chesapeake Bay waters. *Journal of Marine Research* 14:33.
- Chemical Rubber Publishing Co. 1959. *Handbook of chemistry and physics*. 40th ed. Cleveland. 3456 p.
- Clark, George L. and Harry R. James. 1939. Laboratory analysis of the selective absorption of light by sea water. *Journal of the Optical Society of America* 29(2):43-55.
- Dallavalle, J. M. 1948. *Micromeritics*. 2d ed. New York, Pittman. 339 p.
- Dutton, David, M. Parker Givens and Robert E. Hopkins. 1964. Some demonstration experiments in optics using a gas laser. *Spectra-Physics Laser Technical Bulletin*, no. 3:1-5.
- Howerton, L. S. 1966. Company representative, Optical Coating Laboratory, Inc., Santa Rosa, Calif. Personal communication. July, 1966.

- Ivanoff, A., N. G. Jerlov and T. H. Waterman. 1961. A comparative study of irradiance, beam transmittance, and scattering in the sea near Bermuda. *Limnology and Oceanography* 6: 129-148.
- Jenkins, Francis A. and Harvey E. White. 1957. *Fundamentals of optics*. 3rd ed. New York, McGraw-Hill. 637 p.
- Jerlov, Nils G. 1951. Optical studies of ocean waters. In: *Report of the Swedish Deep Sea Expedition, 1947-48*, vol. 3, *Physics and Chemistry* no. 1, p. 1-59.
- _____. 1953. Particle distribution in the ocean. In: *Report of the Swedish Deep Sea Expedition, 1947-48*, vol. 3, *Physics and Chemistry* no. 3, p. 73-77.
- _____. 1955. The particulate matter in the sea as determined by means of the Tyndall meter. *Tellus* 7:218-225.
- _____. 1961. Optical measurements in the N. E. Atlantic. *Meddelander fran oceanografiska institute in Göteborg* 30:1-40.
- Kikuchi, Chihiro and George W. Stroke. (Co-Chrm.) 1965. *Lasers-Theory, technology, and applications*. Course notes for University of Michigan Engineering Summer Conferences, May 10-21, 1965. Various paging. (Course no. 6503) (Processed)
- Pangonis, W. J., W. Heller and A. Jacobson. 1957. *Tables of light scattering functions for spherical particles*. Detroit, Wayne State University Press. 116 p.
- Rempel, Robert C. 1963. Optical properties of lasers as compared to conventional radiators. *Spectra-Physics Laser Technical Bulletin*, no. 1:1-10.
- Spectra-Physics. 1966. *Data sheet on Model 119 single-frequency gas laser*. Mountain View, Calif. 2 p.
- Stroke, George W. 1965. *Optics of coherent and non-coherent electromagnetic radiations*. Ann Arbor, University of Michigan Press. 137 p.
- Tolman, R. C. et al. 1919. Relation between intensity of Tyndall beam and size of particle. *Journal of the American Chemical Society* 41:575-587.

- U.S. National Research Council. 1933. International critical tables of numerical data, physics, chemistry, and technology. New York, McGraw-Hill. Vols. 2, 6, 7.
- Van de Hulst, H. C. 1946. Optics of spherical particles. Amsterdam, N. V. Drukkery, J. F. Duwaer and Zonen. 87 p. (Recherches Astronomiques de l'Observatoire d'Utrecht, vol. 11, pt. 1)
- Vogel, Sy and H. Leon (eds.) 1961. Lasers: Devices and systems - part 1. Electronics, Oct. 27, 1961, p. 39-47.

APPENDIX

APPENDIX

$\beta(\theta)$ remains undetermined as θ approaches 0° and 180° . By using a narrow beam laser and an expansion of the method outlined in Chapter III of the thesis, measurements of $\beta(\theta)$ can be made for $170^\circ < \theta \leq 180^\circ$ and $5^\circ > \theta > 0^\circ$. $\beta(\theta)$ for $\theta = 0^\circ$ cannot be obtained directly, but it can be extrapolated with more accuracy than has been possible up to the present.

Figure I in this section shows the apparatus necessary for studying the backscatter of light from a volume of seawater. A beam-splitter is introduced into the incident beam path in order that one-half of the backscattered light can be reflected out of the incident beam. This apparatus set-up is effectively one-half of an interferometer which separates two light waves (incident and backscattered light waves) traveling in opposite directions. A variable aperture is introduced into the backscattered beam in front of the photodetector. In this position, the variable aperture permits the detector to measure backscatter at angles adjustable from $\theta = 180^\circ$ to $\theta = 170^\circ$ from any scattering point in the scattering volume. If the volume is kept small, the range of θ over which any given aperture setting accepts backscatter is small. Therefore, by careful control of the geometry of the set-up, it should be possible to measure values of $\beta(\theta)$ which are mean values over small ranges of θ , as for example, $\beta(\theta)$ for

$180^\circ > \theta > 179^\circ$. Successive increases in the size of the aperture results in the measurement of means of $\beta(\theta)$ over successively larger angular spreads. By combining the information taken with successive apertures, it should be possible to extract mean values of $\beta(\theta)$ over successive, small angular increments from $180^\circ > \theta > 170^\circ$. It seems possible to replace the variable aperture with a variable ring aperture to accomplish the same result using mechanical means rather than the mathematical recombination suggested above. This would also allow the detection of $\beta(\theta)$ for increments as small as say $172^\circ < \theta < 170^\circ$ and etc. Neshyba (1966) gives one such mathematical treatment of the variable ring aperture technique.¹

Figure II is a diagram of the apparatus which can be used to study the forward scatter of light at scattering angles from about 1° to 5° . Again, a variable aperture is placed in front of the photodetector, but a small light absorbant center for the aperture is necessary in this situation in order to prevent the unscattered laser light beam from entering the photodetector. The light is scattered by the seawater in all directions, and the aperture is variable so as to allow the passage of light scattered at angles from about 1° to 5° . Again $\beta(\theta)$ can be found for θ increments of $1^\circ < \theta < 1.5^\circ$ and etc.

It should be stated that Spilhaus (1965) employed a similar

¹Neshyba, S. J. 1966. Proposal for Research in Direct Forward Scatter of Light by Particulates in the Sea. NSF Grant GA-545.

scheme to measure forward scatter at angles of 1° - 5° . But he did not employ a variable aperture and hence was unable to measure $\beta(\theta)$ for incremental angular spreads smaller than about 5° in width.

Thus, $\beta(\theta)$ can be measured for all backscatter angles, and its value in the forward directions can be determined for angles approaching $\theta = 0^\circ$. Having a more complete graph of $\beta(\theta)$ versus θ allows a more accurate extrapolation of $\beta(0^\circ)$ to be made. As a result, the total scattering coefficient, b , is more accurately determinable. Again it must be emphasized that $\beta(\theta)$ for $\theta = 0^\circ$ is not directly attainable.

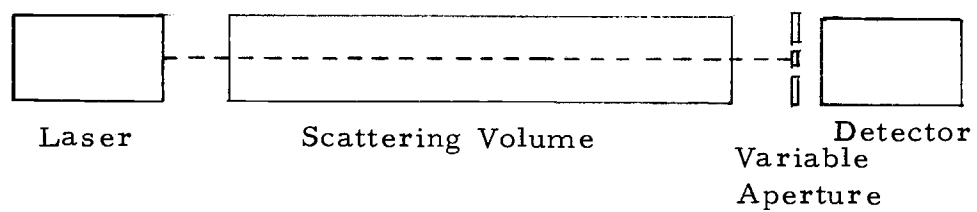


Figure II. Near Forward Scatter Apparatus

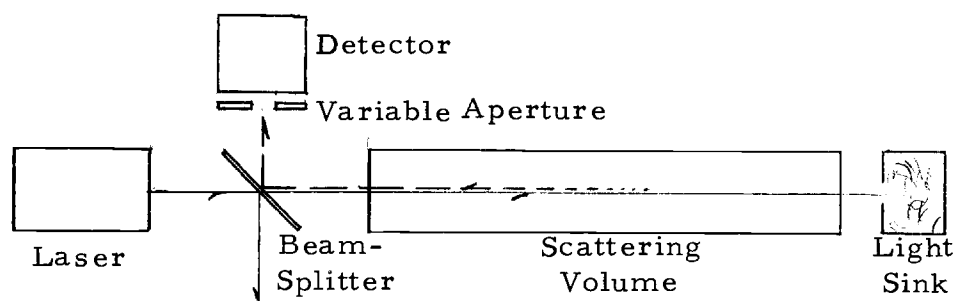


Figure I. Backscatter Apparatus